

## Meteor shower output caused by comet 15P/Finlay

J Vaubaillon, A Egal, J Desmars, Kevin Baillie

► **To cite this version:**

J Vaubaillon, A Egal, J Desmars, Kevin Baillie. Meteor shower output caused by comet 15P/Finlay. WGN, Journal of the International Meteor Organization, International Meteor Organization, 2020. hal-03017579

**HAL Id: hal-03017579**

**<https://hal.archives-ouvertes.fr/hal-03017579>**

Submitted on 21 Nov 2020

**HAL** is a multi-disciplinary open access archive for the deposit and dissemination of scientific research documents, whether they are published or not. The documents may come from teaching and research institutions in France or abroad, or from public or private research centers.

L'archive ouverte pluridisciplinaire **HAL**, est destinée au dépôt et à la diffusion de documents scientifiques de niveau recherche, publiés ou non, émanant des établissements d'enseignement et de recherche français ou étrangers, des laboratoires publics ou privés.

# Meteor shower output caused by comet 15P/Finlay

*J. Vaubaillon*<sup>1</sup>, *A. Egal*<sup>2</sup>, *J. Desmars*<sup>3</sup>, *K. Baillié*<sup>4</sup>

Theoretical work on the meteoroid stream ejected by comet 15P/Finlay predicts multiple outbursts in 2021 in agreement with previous authors. This work predicts the first outburst to happen around 2021-09-29T08:35 UT, for a radiant located at  $\alpha = 260.8$  deg  $\delta = -57.4$  deg and will be best visible from New-Zealand. The second will happen on 2021-10-07T00:35 UT, followed by a third on 2021-10-07T03:55 UT. They will be best visible from the tip of Antarctica or Tierra Del Fuego (Argentina). The level of each outburst is evaluated based on the photometry of the comet, which is known to have experienced some outbursts, but is less certain than the timing of each event.

## 1 Introduction

Meteor shower outburst are now commonly predicted (Vaubaillon et al., 2019). If the timing of occurrence of a meteor shower is pretty reliable, the level of an outburst is still today much harder and hazardous to assess. Recent success include the  $\alpha$ -Monocerotids (Jenniskens and Lyytinen, 2019a,b). The outburst was on time but the level was much less than expected. Though some observers might be disappointed, this also raises exciting curiosity regarding this field of research that still needs input of new ideas, models and theories to better reproduce natural phenomena.

One of the current challenges is to predict the occurrence of a shower that has never been observed before. This paper presents the prediction of a meteor shower outburst caused by comet 15P/Finlay, known to be a Near-Earth object. Despite a promising orbital configuration, no meteor shower associated with 15P/Finlay has been found in observation databases so far (or at least prior to 2000, cf. Beech et al., 1999). Because a low encounter velocity with Earth, meteors produced by comet Finlay will necessarily be faint and hardly detectable by meteor observers. More recently, a search among the records of the Canadian Meteor Orbit Radar (CMOR) database did not reveal the existence of any past "Finlayid" activity (Ye et al., 2015). However, Ye et al. (2015) reported a possible southern shower on the 6th-7th of October 2021, based on their own work as well as those performed by Mikiya Sato<sup>5</sup>, Mikhail Maslov<sup>6</sup>, as well as Shanov and Dubrovski (cited in Jenniskens, 2006). These predictions are reminded in Table 1.

In this paper we present the result of our modelling of meteoroid streams ejected by comet 15P/Finlay during its latest apparitions. We predict a meteor shower in 2021, caused by the trails ejected in 2008 and 2014. In Section 2, the orbital evolution of 15P/Finlay is investigated. Section 3 present our meteor shower forecast. These predictions are finally discussed in Section 4.

## 2 Comet 15P/Finlay

Comet Finlay is a Jupiter family comet (period of 6.5 years) discovered in 1886 by W.H. Finlay, and observed during 13 passages in total. Its orbit is therefore well known and constrained for this period of time (see table 2). The nucleus of the comet was estimated to  $0.92 \pm 0.05$  km (Fernández et al., 2013). Ishiguro et al. (2016) points out that the comet is known to show irregular activity and to experience several activity outburst, the latest happening in 2014 and 2015. They found a dust production rate of  $10^8 - 10^9$  kg per outburst for less than mm-size particles. This is comparable to the production of comet 55P/Swift-Tuttle, parent body of the Leonids meteor shower (Vaubaillon et al., 2005b). Therefore the comet is theoretically able to produce a meteor shower at Earth, provided our planet enters the meteoroid stream.

Before performing any meteor shower prediction, the ephemeris of the parent body must be established, either from observations or from numerical integration of its orbit as a function of time. We therefore start investigating the orbital stability of 15P/Finlay. A thousand of comet clones are generated using the covariance matrix provided in JPL 142/2, corresponding to the solution of Table 2. Each clone of the comet is integrated backwards for more than 500 years, using a 15<sup>th</sup> order RADAU integrator (Everhart, 1985) with an external time step of 1 day. The force model for the integration includes the gravitational attraction of the Sun, the eight planets of the Solar System, the Moon and Pluto, as well as the relativistic corrections to bring to the trajectories. Non-gravitational forces (NGF) due to cometary outgassing were optionally included.

Figure 1 describes the past orbital evolution of the swarm of 15P clones. For each orbital element, the evolution of the nominal clone when considering (grey solid line) or excluding (black curve with open circles) cometary non-gravitational forces is presented. Both trajectories reflect the influence of jovian perturbations on the global evolution of the comet. The discrepancy between both NGF models becomes significant after 330 years of integration.

The dispersion of the swarm of clones, represented by the standard deviation of each orbital element, is illustrated by the limiting lines (black solid curves) above and below the nominal clone solution without NGF of Figure 1. Sudden and significant variations of the clones standard deviation are mainly induced by close encounters with planets,

<sup>5</sup> <https://groups.yahoo.com/neo/groups/meteorobs/conversations/messages/4030> counter=1, accessed on the 29th Nov. 2019

<sup>6</sup> web page cited by Ye. et al, 2015 inaccessible on the 29th Nov. 2019

<sup>1</sup>IMCCE, Observatoire de Paris, PSL Research University, CNRS, Sorbonne Université, UPMC Univ. Paris 06, Univ. Lille., France  
Email: jeremie.vaubaillon@obspm.fr

<sup>2</sup>The University of Western Ontario, London, Ontario, Canada ; Centre for Planetary Science and Exploration, The University of Western Ontario, London, Ontario N6A 5B8, Canada

Email: auriane.egal@obspm.fr

<sup>3</sup>Institut Poytechnique des Sciences Avancées IPSA, 63 boulevard de Brandebourg, F-94200 Ivry-sur-Seine, France, IMCCE, Observatoire de Paris,

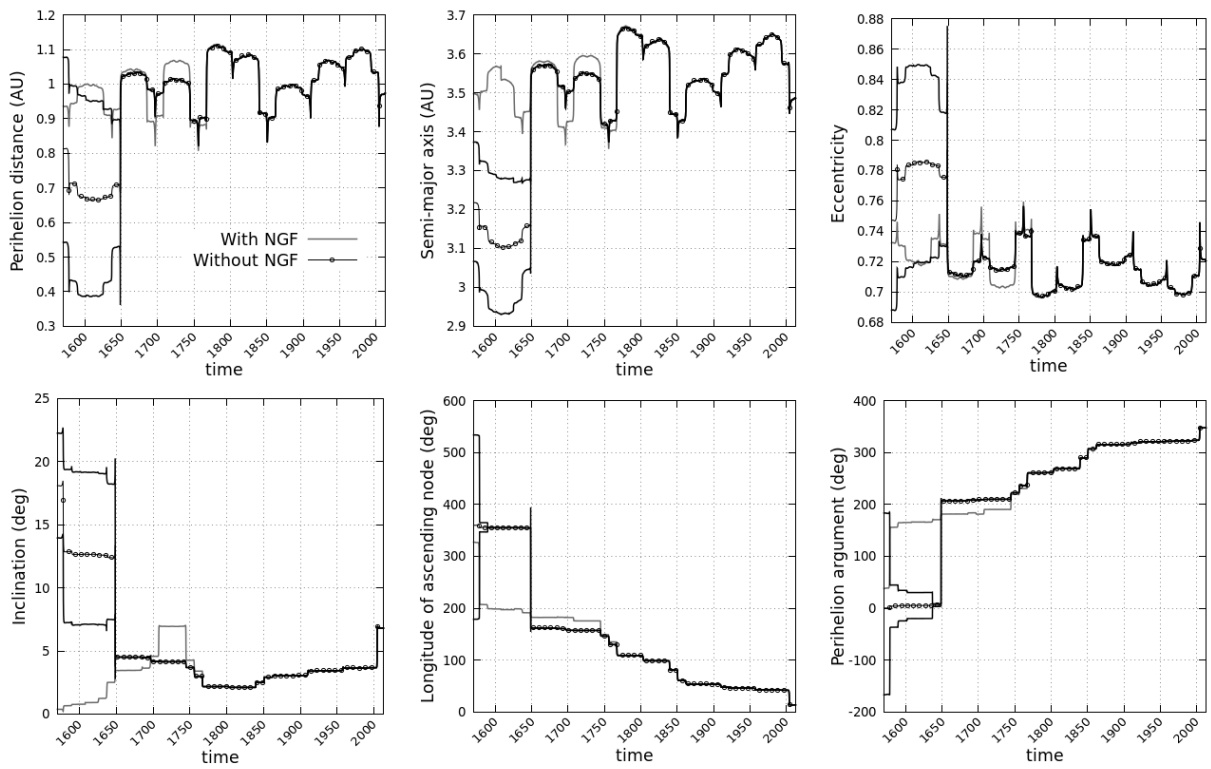


FIGURE 1 – Dynamical evolution of comet 15P/Finlay over 500 years. The orbital evolution of the nominal clone is represented by the grey solid line (integration with NGF) or black dotted line (integration without NGF). The clones standard deviation  $\sigma$  is illustrated by the black solid lines above and below the nominal solution without NGF (nominal solution  $\pm 1\sigma$ ).

Modeler	Peak Time	Radiant	vg	ZHR
Maslov	2021 Oct. 7, 01:19	255.8°, -48.3°	10.7	5-50
Sato	2021 Oct. 7, 01:10	255.7°, -48.4°	10.7	...
Ye	2021 Oct. 7, 00:34-01:09	255.6°, -48.4°	10.7	...
Ye	2021 Oct. 6, 21:59-22:33	256.3°, -48.5°	10.7	...

TABLE 1 – Previous predictions of the 2021 encounter with 15P/Finlay’s meteoroid trails summarized in Table 4 of Ye et al. (2015)

Epoch	2013-Apr-24 TDB
semi-major axis	3.4867 AU
eccentricity	0.7204
inclination	6.8037°
node	13.8006°
argument of perihelion	347.5656°
mean anomaly	267.3628°

TABLE 2 – Orbital elements of comet 15P/Finlay, from JPL/HORIZONS.

resulting in abrupt dispersion of the simulated particles. After a first increase around 1744 AD, the clones dispersion increases drastically around 1648 AD because of a close encounter with Jupiter. Before this date, the comet ephemeris is highly uncertain and should not be considered without a careful analysis.

### 3 Predictions for 2021

In order to perform the meteor shower prediction we used the models developed by Vaubaillon et al. (2005a); Vaubaillon (2017) (hereafter called "JV2005") and Egal et al. (2018, 2019) (hereafter "AE2019"). The two sets of simulations consider every perihelion passage of the comet between 1886 and 2014, and 1905 to 2014 respectively. As concluded in Section 2, the ephemeris of the comet is reliable over this time span. The simulations involved 570 000 and 3,468,000 particles respectively.

Figure 2 presents a compilation of the nodal crossing location of all the particles crossing the ecliptic plane in 2021. Different colours refer to different ejection epochs. If no enhanced activity can be directly predicted from this Figure (most of the particles cross the ecliptic plane when the Earth is far from their location), it illustrates the high perturbations meteoroid trails suffer after their ejection.

In the line of Jenniskens (2006), Maslov (web page no longer available) and M. Sato<sup>7</sup> we find that the Earth will encounter the meteoroid stream ejected by comet 15P/Finlay in 2021. However we also find multiple outbursts of varying strength and time.

Figures 3, 4 and 5 show the location of the nodes of the meteoroids ejected during the 1995, 2014 and 2008 passages of the comet, respectively responsible for the first, second and third peaks, obtained from the method of JV2005. The distribution of radiant are shown in Fig 6, 7 and 8. A summary of the encounter circumstances is presented in Table 3.

For comparison sake, Figure 9 shows the structure of the stream close to Earth around the expected peaks obtained with the AE2019 model. Particles crossing the ecliptic plane at less than 0.001 AU from Earth’s orbit, and within  $\pm 3$  days of the planet’s location (coloured particles) were retained for this analysis. The encounter geometry with the 1995, 2008 and 2014 trails is similar to what observed in Figures 3, 4 and 5. The apparent weaker density of particles in Figure 9 is mainly due to a more restrictive selection of the simulated meteoroids. In this model, the 1995 trail is expected to approach Earth in September 2021, producing a weak activity around September 28 to 29 ( $L_{\odot}$  from 185.46° to 186.32°). The 2008 and 2014 trail are expected to produce a stronger activity on October 6 to 7, 2021. As found with the JV2005 model, the 2014 trail is concentrated at the beginning of October 7, producing a sharper peak of activity. From a first approximation, the 2008 trail might be involved in a weak activity a few hours later. In these simulations, the existence of a fourth wide and low activity caused by the 2002 trail is also found. This peak occurs on October 8th, after a slow rise of activity lasting 3 days in total. The level is less than the peak caused by the 2008 trail.

The accurate prediction of a shower duration, peak time and intensity depends on several criteria, like the threshold distance with Earth’s orbit, the relative time passage with the planet or the weighting scheme applied to the simula-

7. <https://groups.yahoo.com/neo/groups/meteorobs/conversations/messages/44030?withcounter=1>, accessed on the 29th Nov. 2019

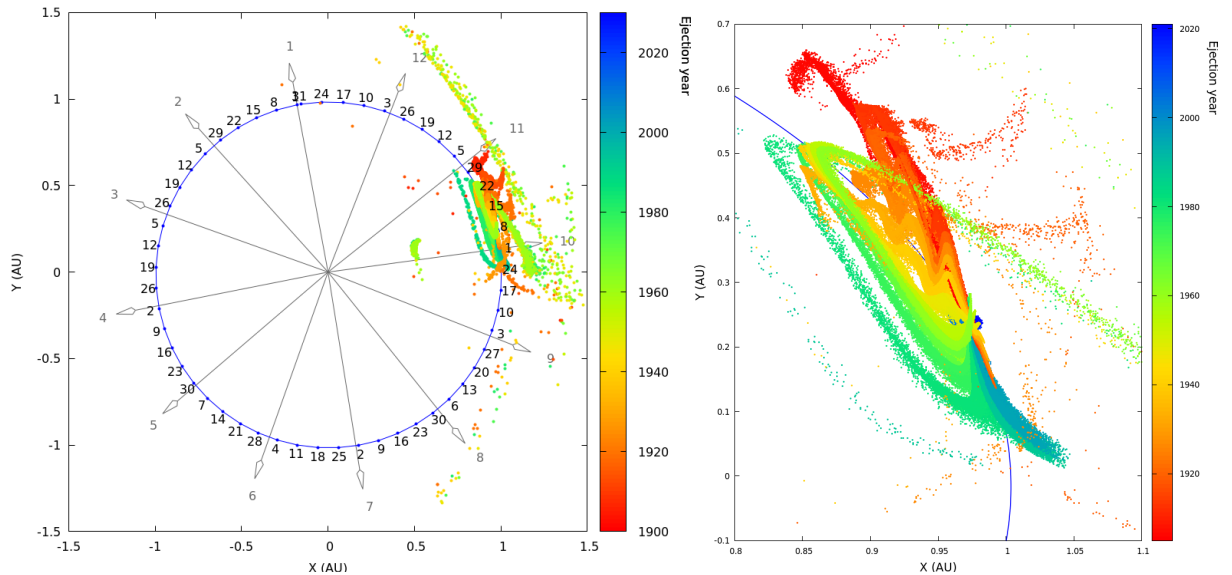


FIGURE 2 – Location of meteoroids ejected from 15P/Finlay crossing the ecliptic plane in 2021 (from model AE2019). Different colours refer to different ejection dates. Grey arrows point towards the Earth’s location at the beginning of each month (varying from 1 to 12). The position of the planet every 7 days from these dates are indicated by blue dots and their corresponding number.

TABLE 3 – Circumstances of encounter between the Earth and meteoroid trails ejected from comet 15P/Finlay (from model JV2005). trail: year of ejection of the considered trail intersecting the Earth in 2021. dist: mean distance of the trail to the Earth. SolLong: Solar Longitude at the time of maximum ;  $V_{geo}$ : expected geocentric velocity ;  $\alpha$ ,  $\delta$ : coordinates and standard deviation of the radiant ; ZHR: zenithal hourly rate (see also section 4) ; conf\_id : confidence index as defined by Vaubaillon (2017).

trail year	dist AU	SolLong deg	date UT	$\alpha$ deg	$\delta$ deg	$V_{geo}$ $km.s^{-1}$	ZHR $hr^{-1}$	conf_id
1995	0.00125	186.072	2021-09-29T08:35	$260.8 \pm 0.9$	$-57.4 \pm 0.5$	10.807	13	SY00/ICE0.00
2008	-0.00143	193.728	2021-10-07T03:55	$254.5 \pm 1.0$	$-48.3 \pm 0.2$	10.730	41	SY00/ICE0.00
2014	0.00028	193.674	2021-10-07T00:35	$255.5 \pm 0.8$	$-48.3 \pm 0.6$	10.752	178	SY00/ICE0.00

ted meteoroids (cf. Vaubaillon et al., 2005a or Egal et al., 2019). In this analysis, this process is even harder since no meteor shower associated to comet 15P/Finlay has been observed in the past. Figure 10 illustrates how the duration and shape of the shower intensity profile evolve with the weights applied to the particles. The grey curve represents the flux variation when the same weight is attributed to all the particles (called "unweighted" solution). The black dotted curve represents the output of Egal et al., 2019 weighting scheme for a meteoroids size distribution index at ejection of 2.5 (called "weighted" solution). Each peak time is conserved after the application of the different weights. However, the duration and shape of the 6-7 October activity differ from one solution to another, and the suspected fourth peak caused by the 2002 trail on October 8 disappears in the weighted solution. The relative contribution of each trail to the profile is presented in Figure 11. We see

that our weighting scheme increased the estimated intensity of the 2014 and 1995 trails, while lowered down the contribution of the 2008 and 2002 trails.

From these simulations, four peaks of activity might be observable in September-October 2021, around the solar longitudes  $186.077^\circ$  (1995 trail),  $193.677^\circ$  (2014 trail),  $193.785^\circ$  (2008 trail) and  $194.527^\circ$  (2002 trail). The main activity is expected to be caused by the 2014 trail, which should be at least twice as large as all the other peaks. However, no reliable ZHR can be estimated from this model without a proper calibration based on meteor measurements at this stage. For more realistic estimates of the ZHR, the reader is referred to the values presented in Table 3, where the simulated meteoroid flux obtained with JV2005 model has been calibrated on the photometry of the comet. However, even with such a model, the size distribution of  $> 100 \mu m$  is unknown since visible photometry of comet

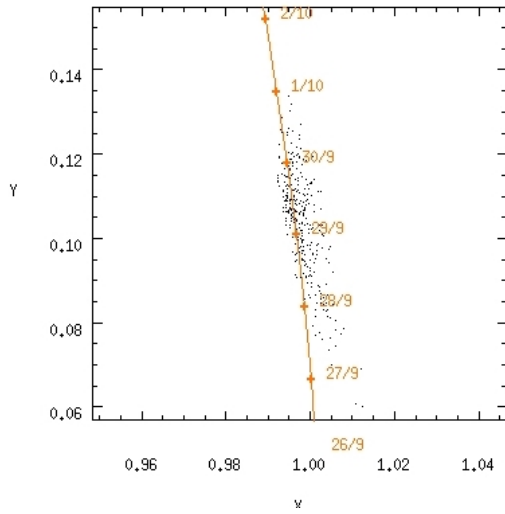


FIGURE 3 – Meteoroid trail ejected in 1995 configuration with respect to the Earth (from model JV2005), causing the first peak of the 2021 meteor outburst caused by comet 15P/Finlay.

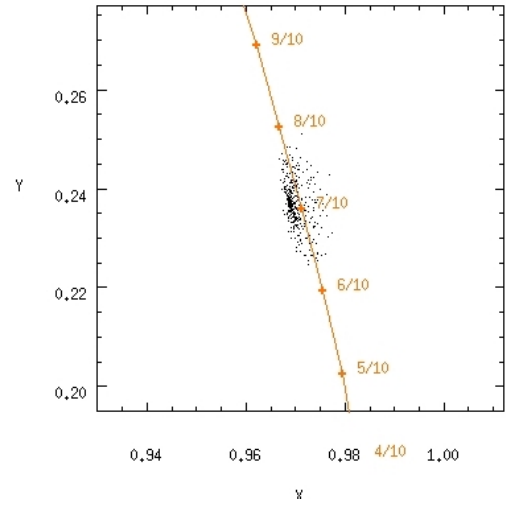


FIGURE 5 – Meteoroid trail ejected in 2008 configuration with respect to the Earth, causing the third peak of the 2021 meteor outburst caused by comet 15P/Finlay.

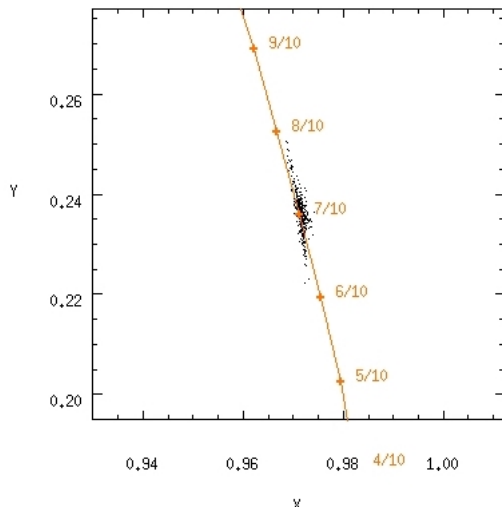


FIGURE 4 – Meteoroid trail ejected in 2014 configuration with respect to the Earth (from model JV2005), causing the second peak of the 2021 meteor outburst caused by comet 15P/Finlay.

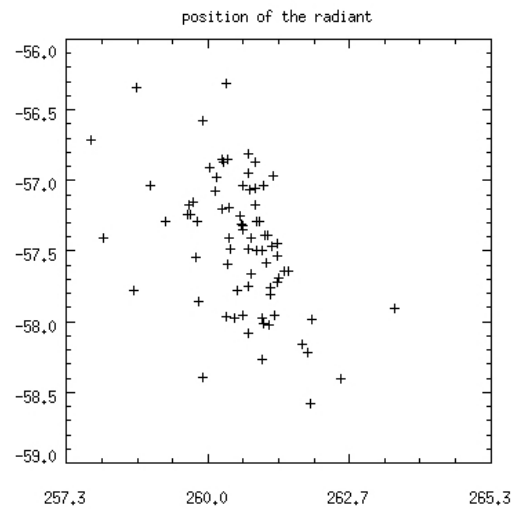


FIGURE 6 – Theoretical radiant distribution of the first peak (from model JV2005).

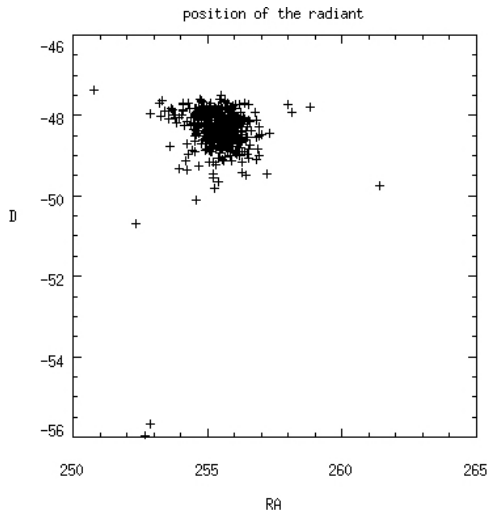


FIGURE 7 – Theoretical radiant distribution of the second peak (from model JV2005).

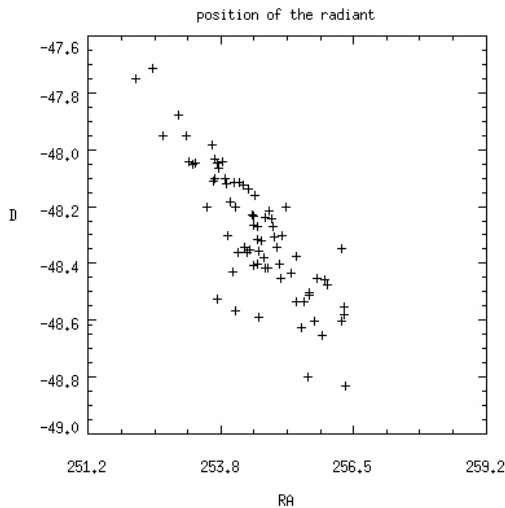


FIGURE 8 – Theoretical radiant distribution of the third peak (from model JV2005).

coma is performed for  $\approx \mu\text{m}$ -size particles.

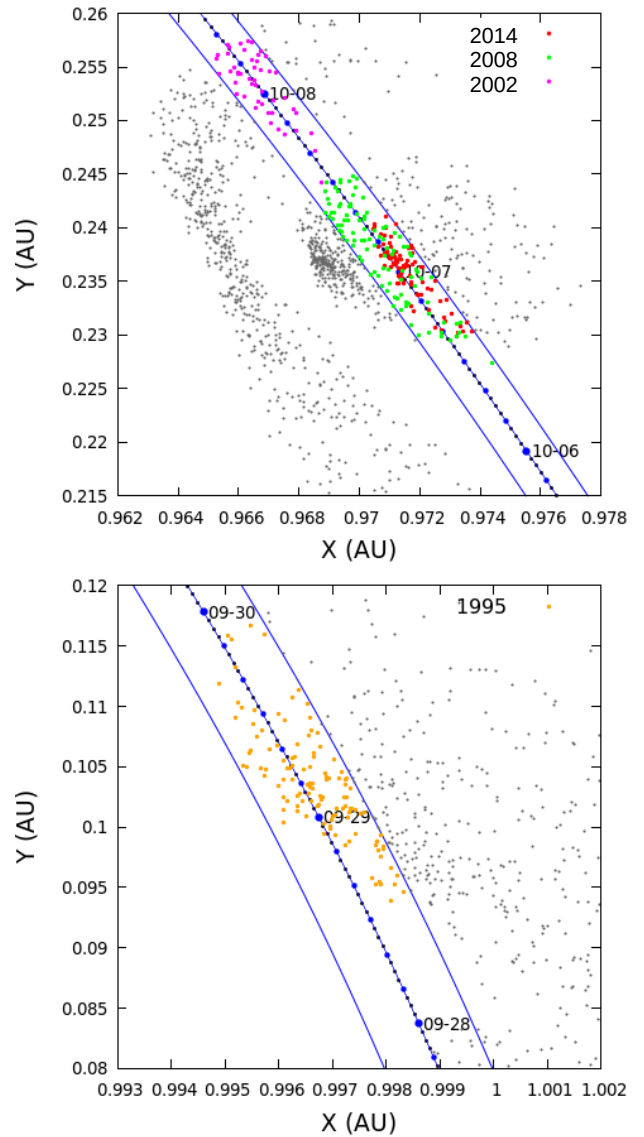


FIGURE 9 – Nodal crossing location of meteoroids simulated using AE2019 model around September 9, 2021 (bottom panel) and October 7, 2021 (top panel). The dashed blue curve represents the Earth's successive locations in 2021, while solid lines mark the region considered for the analysis. Meteoroids retained are colour-coded in function of their ejection epoch.

### 3.1 Shower visibility geometry

The mean location of the radiants puts the shower in the constellation of Ara. The orientation of the Earth and the location of the sub-radiant points are shown in Figs 12, 13 and 14. The location of the radiants and the corresponding time of maxima are provided in Table 3.

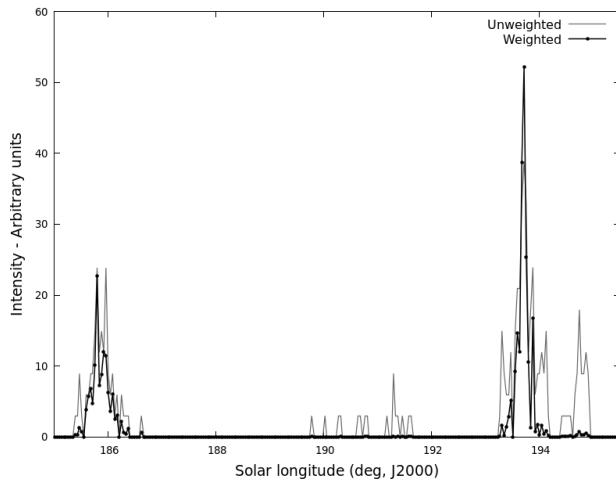


FIGURE 10 – Influence of the weighting scheme on the activity profile of the shower (from model AE2019).

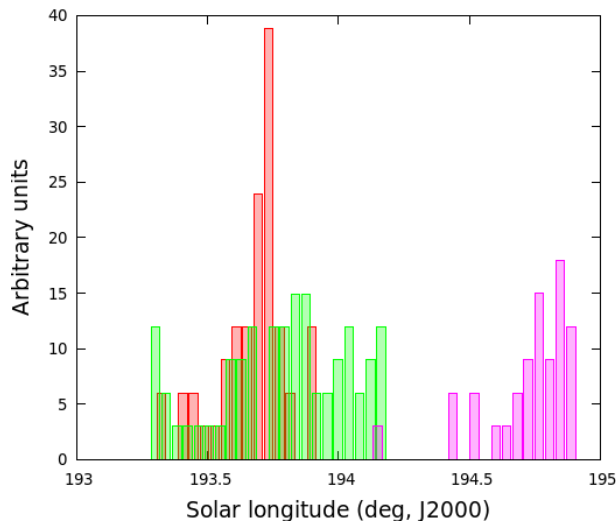
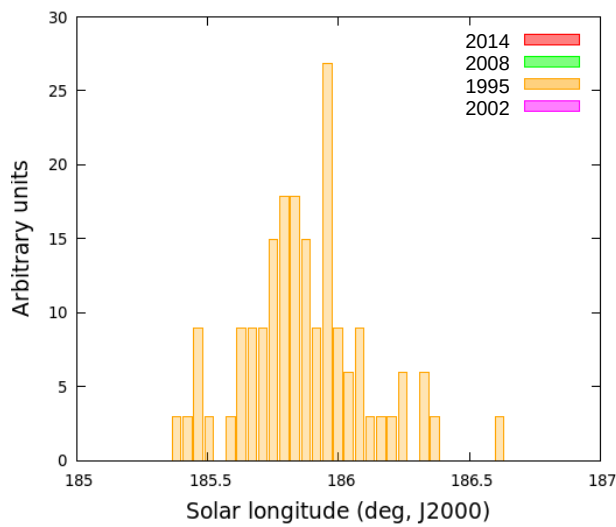


FIGURE 11 – Relative contribution of each trail to the un-weighted profile of Figure 10 (from model AE2019).

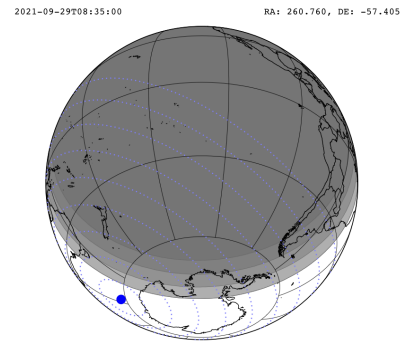


FIGURE 12 – Sub-radiant location of the first peak (blue dot). Earth surface in the night is represented in gray colour with different level of grey corresponding to civil, nautical and astronomical twilights. The dotted blue lines represents the isoelevation lines of the radiant every 10 degrees.

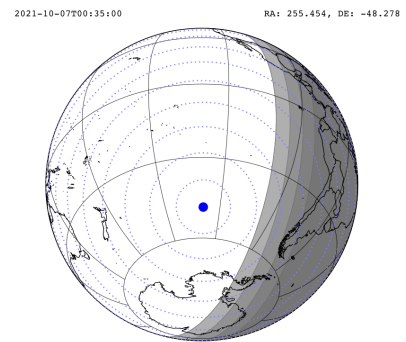


FIGURE 13 – Sub-radiant location of the second peak. See Fig. 12.

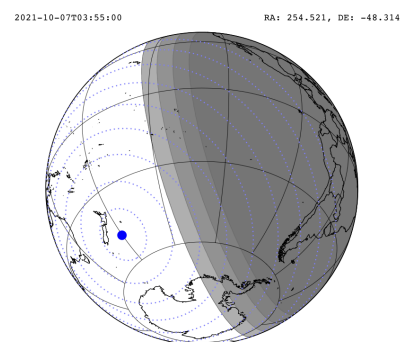


FIGURE 14 – Sub-radiant location of the third peak. See Fig. 12

## 4 Discussion and conclusion

The meteors will enter the Earth at a very low velocity of  $10.8 \text{ km.s}^{-1}$ , so only the largest ones will cause visible



meteors. From Fig.3 we can forecast that the activity of the first peak will be broad, lasting nearly an entire day. This will ease its observation from nearly any point in the Southern hemisphere. However, an expected  $ZHR$  of  $13 \text{ hr}^{-1}$  (table 3) will make it hard to distinguish from sporadic background. Ideally a global effort to follow the outburst from beginning to end is required. The peak will be best observed at its central part from New-Zealand, as seen in Fig 12.

Presumably the 2nd and 3rd peaks will be easier to spot w.r.t. sporadic background thanks to a higher  $ZHR$ . They might both be observed from a single area located either at the Northern-most tip of Antarctica or the Southern-most tip of the American continent (Fig 13 and 14).

The ratio between  $< 1 \text{ mm}$  and  $> 1 \text{ mm}$  simulated particles for model #1 are: 10:1 for the 1995 trail, 100:1 for the 2008 trail, and nearly 1:1 for the 2014 trail. The extreme low velocity will affect the visibility of the showers in the visible spectrum. As a consequence, the most likely visible shower is that caused by the 2014 trail.

Observers should keep in mind that the level of the showers have large uncertainties since this will be the first observed meteor shower from comet 15P/Finlay. The comet outburst in 2014 makes the predicted third peak the most exciting outburst to observe. However the two other peaks are mandatory to record in order to quantify the change of activity of the comet before and after the outburst. Although the comet outburst in 2014 was witnessed and recorded, the exact amount of large meteoroids (causing visible meteors) is unknown.

We conclude as a call to observers to report their measurements to the International Meteor Organization <sup>8</sup>.

## 5 Acknowledgements

Part of the calculations used the CINES supercomputer facility, France. Simulations performed by A. Egal were supported in part by NASA Meteoroid Environment Office under cooperative agreement 80NSSC18M0046 and contract 80MSFC18C0011.

## Références

Beech, M., Nikolova, S., and Jones, J. (1999). The ‘silent world’ of Comet 15P/Finlay. *MNRAS*, 310(1):168–174.

Egal, A., Wiegert, P., Brown, P. G., Moser, D. E., Campbell-Brown, M., Moorhead, A., Ehlert, S., and Moticska, N. (2019). Meteor shower modeling: Past and future Draconid outbursts. *Icarus*, 330:123–141.

Egal, A., Wiegert, P., Brown, P. G., Moser, D. E., Moorhead, A. V., and Cooke, W. J. (2018). The Draconid Meteoroid Stream 2018: Prospects for Satellite Impact Detection. *ApJ*, 866(1):L8.

Everhart, E. (1985). An efficient integrator that uses Gauss-Radau spacings. *International Astronomical Union Colloquium*, 83:185–202.

Fernández, Y. R., Kelley, M. S., Lamy, P. L., Toth, I., Groussin, O., Lisse, C. M., A’Hearn, M. F., Bauer, J. M., Campins, H., Fitzsimmons, A., Licandro, J., Lowry, S. C., Meech, K. J., Pittichová, J., Reach, W. T., Snodgrass, C., and Weaver, H. A. (2013). Thermal properties, sizes, and size distribution of Jupiter-family cometary nuclei. *Icarus*, 226(1):1138–1170.

Ishiguro, M., Kuroda, D., Hanayama, H., Kwon, Y. G., Kim, Y., Lee, M. G., Watanabe, M., Akitaya, H., Kawabata, K., Itoh, R., Nakaoka, T., Yoshida, M., Imai, M., Sarugaku, Y., Yanagisawa, K., Ohta, K., Kawai, N., Miyaji, T., Fukushima, H., Honda, S., Takahashi, J., Sato, M., Vaubaillon, J. J., and Watanabe, J.-i. (2016). 2014-2015 Multiple Outbursts of 15P/Finlay. *AJ*, 152(6):169.

Jenniskens, P. (2006). *Meteor Showers and their Parent Comets*.

Jenniskens, P. and Lyytinen, E. (2019a). Alpha Monocerotids 2019. *Central Bureau Electronic Telegrams*, 4692:1.

Jenniskens, P. and Lyytinen, E. (2019b). Alpha Monocerotids Meteors 2019. *Central Bureau Electronic Telegrams*, 4699:1.

Vaubaillon, J. (2017). A confidence index for forecasting of meteor showers. *Planet. Space Sci.*, 143:78–82.

Vaubaillon, J., Colas, F., and Jorda, L. (2005a). A new method to predict meteor showers. I. Description of the model. *A&A*, 439(2):751–760.

Vaubaillon, J., Colas, F., and Jorda, L. (2005b). A new method to predict meteor showers. II. Application to the Leonids. *A&A*, 439(2):761–770.

Vaubaillon, J., Neslušan, L., Sekhar, A., Rudawska, R., and Ryabova, G. O. (2019). *From Parent Body to Meteor Shower: The Dynamics of Meteoroid Streams*, page 161.

Ye, Q.-Z., Brown, P. G., Bell, C., Gao, X., Mašek, M., and Hui, M.-T. (2015). Bangs and Meteors from the Quiet Comet 15P/Finlay. *ApJ*, 814(1):79.

<sup>8</sup>. [www.imo.net](http://www.imo.net)